Research Paper

EARTHQUAKE SPECTRA

Earthquake Spectra
1–27

DOI: 10.1177/87552930221076870
journals.sagepub.com/home/eqs
SAGE

Investment planning for earthquake-resilient electric power systems considering cascading outages

Boyu Cheng[1], Linda Nozick[1], and Ian Dobson[2]

Abstract

Earthquakes cause outages of power transmission system components due to direct physical damage and also through the initiation of cascading processes. This article explores what are the optimal capacity investments to increase the resilience of electric power transmission systems to earthquakes and how those investments change with respect to two issues: (1) the impact of including cascades in the investment optimization model and (2) the impact of focusing more heavily on the early stages of the outages after the earthquake in contrast to more evenly focusing on outages across the entire restoration process. A cascading outage model driven by the statistics of sample utility data is developed and used to locate the cascading lines. We compare the investment plans with and without the modeling of the cascades and with different levels of importance attached to outages that occur during different periods of the restoration process. Using a case study of the Eastern Interconnect transmission grid, where the seismic hazard stems mostly from the New Madrid Seismic Zone, we find that the cascades have little effect on the optimal set of capacity enhancement investments. However, the cascades do have a significant impact on the early stages of the restoration process. Also, the cascading lines can be far away from the initial physically damaged lines. More broadly, the early stages of the earthquake restoration process is affected by the extent of the cascading outages and is critical for search and rescue as well as restoring vital services. Also, we show that an investment plan focusing more heavily on outages in the first 3 days after the earthquake yields fewer outages in the first month, but more outages later in comparison with an investment plan focusing uniformly on outages over an entire 6-month restoration process.

Keywords

Power system, earthquake, optimization, restoration, algorithm

Date received: 21 February 2021; accepted: 11 January 2022

[1]School of Civil and Environmental Engineering, Cornell University, Ithaca, NY, USA
[2]Department of Electrical and Computer Engineering, Iowa State University, Ames, IA, USA

Corresponding author:
Boyu Cheng, School of Civil and Environmental Engineering, Cornell University, Ithaca, NY 14853, USA.
Email: bc652@cornell.edu

Introduction

Earthquakes can cause substantial damage to electric power systems. For example, the 1994 Northridge earthquake hit Los Angeles causing 2.5 million people to lose electric power (Dong et al., 2004). The damage to fossil fuel plants, transmission lines, substations and distribution lines caused by the Hanshin-Awaji earthquake led to an outage of over 2800 MW and affected almost 2.6 million customers (Noda, 2001). In 2008, the Wenchuan earthquake hit the Sichuan province in China. In addition to substantial casualties, the power transmission network and local distribution systems sustained heavy damages. The estimated repair cost was about US$4.6 billion and the economic impact was valued as US$1.56 billion (Eidinger, 2009). In 2011, the earthquake in Christchurch, New Zealand destroyed 50% of 66 kV cables, 15% of 11 kV cables, and four substations of the power distribution system (Massie and Watson, 2011). On November 14, 2016, an earthquake with a moment magnitude of 7.8 occurred in Kaikoura, New Zealand. Around 7000 homes and businesses lost electricity supply (Liu et al., 2017).

Physical damage to electric power system components caused by earthquakes also triggers additional outages through a variety of mechanisms, including system safeguards that protect equipment from physical damage. These cascading outages are a series of dependent outages that successively weaken the power system and can cause widespread blackouts (Baldick et al., 2008). On August 14, 2003, a cascading blackout in North America affected about 50 million people across several states (US–Canada Power System Outage Task Force, 2004). In September 2003, a power outage occurred initially in Switzerland and spread to a large region of Italy via cascading failures (Dong et al., 2004).

This article focuses on long-term investment planning in the electric power system to mitigate the impacts of earthquakes. The impacts of cascading outages are also integrated into this analysis. The earthquake causes physical damage to power system components whereas the cascade causes equipment to trip out. Cascade-generated outages can have a much larger geographic extent than the outages produced by initial physical damages. When considering this question, it is important to realize that in the immediate aftermath of an earthquake there are life safety concerns as well as important restoration activities for other lifeline systems. An inability to provide electric power can severely hamper these efforts, especially when the blackout is widespread. Hence, the importance of restoring electrical power quickly to support these restoration activities leads to the exploration of the differences in investment plans that can be generated if more attention is focused on the few days right after the earthquake in contrast to focusing more evenly over the entire repair horizon for the electric power system.

The primary contributions of this study are (1) the integration of cascade effects into the investment planning model for mitigating the impacts of earthquake damage on the electric power transmission system and (2) understanding the differences in the recommendations if we more heavily weight unserved demand in the first days after the event in contrast to when we do not do that. By implementing the model on the Eastern Interconnect grid,[1] where the seismic hazard mainly stems from the New Madrid Seismic Zone, the results indicate that it is not necessary to include the cascades in the investment planning. However, to understand the true impacts of the earthquakes, cascading must be included. If cascading is ignored the availability of power in the few days after the earthquake will be significantly overestimated and the geographic extent of the outages will be underestimated. A secondary contribution of this study is the empirical demonstration that if the investment plan is developed focusing more heavily on outages in the first few days after

the earthquake, the network will have fewer outages in the few days after the earthquake, but more outages later in comparison with developing the investment plan by focusing more evenly on outages across the entire restoration process.

The original contributions of this work include the integration of DC load flow power systems analysis with probabilistic cascading analysis at the scale of a large interconnection network model (with 14,957 buses, 16,435 lines, and 6981 transformers) to optimize investments in earthquake resilience. The high-level probabilistic cascading analysis is suitable for the scale of the network, is driven by outage data routinely collected by utilities, and, together with the variant of this probabilistic cascading analysis recently published in the work of Kelly-Gorham et al. (2020), is a novel approach in both earthquake research and blackout research. Moreover, the probabilistic cascading analysis in this article uses stratified sampling to efficiently sample from the rarer, high-impact cascades.

The remainder of this article is organized as follows. The next section describes the relevant literature. The third section describes the models used to conduct this analysis. The fourth section describes the case study. The final section discusses opportunities for future research.

Literature review

The relevant literature is concentrated in two main areas. The first area is modeling to support the mitigation of the impacts of earthquakes on power systems. The second area is the modeling of cascading outages. The remainder of this section will focus on these two areas in turn.

Historically, when focusing on designing and improving the performance of the power systems, researchers focus on the reliability of the average performance (Lagos et al., 2019). For instance, the system average interruption frequency index (SAIFI) and system average interruption duration index (SAIDI) are two common indicators of reliability in power distribution systems (Liu, 2015). However, in these traditional reliability-driven approaches, high-impact and low-probability events (HILP), such as earthquakes are not always considered (Lagos et al., 2019). Therefore, the concept of resilience has been introduced for the design and improvement of the performance of the power systems. Stankovic (2018) defined resilience as the ability to withstand and reduce the magnitude and/or duration of disruptive events, which includes the capability to anticipate, absorb, adapt to, and/or rapidly recover from such an event.

Two common directions are often used in developing the strategies or investment plans for mitigating the impact of earthquakes and improving the resilience of power systems. The first direction is to develop index measurement to locate the critical components in power systems for upgrades or for hardening. Vanzi (2000) developed a strategy for optimizing the structural upgrading of electric power systems. In this strategy, a new index is created to find the critical nodes in the system. Shumuta (2007) developed four indices for upgrading substation equipment. The first and second indexes focus on the equipment resistance against earthquakes, the third index focuses on the seismic performance, and the fourth index focuses on the cost-effectiveness of the equipment. A case study was conducted on a hypothetical electric power system in the Nagoya region of Japan. Espinoza et al. (2020) have developed an electric power system equipment criticality assessment methodology based on risk and resilience. This methodology has been tested on the electric power system in Northern Chile against an inventory of 90,000 earthquake scenarios.

The second direction researchers have explored is the creation of mathematical programming models to optimize investment plans to mitigate the impact of earthquakes and promote the resilience of power systems. Romero et al. (2013) developed a two-stage stochastic programming model to optimize the expansion of transmission lines and generation capacity to increase the resilience of power systems under earthquake hazards. The same research team also proposed a two-stage stochastic program model for optimizing the selection of transmission lines and substations for reinforcement to mitigate the impact of earthquakes (Romero et al., 2015). Nagarajan et al. (2016) optimized the upgrade options for transmission systems to improve the system's resilience. A two-stage mixed-integer stochastic model was built for the problem and the upgrade option included adding new lines, adding flexible alternating current transmission system devices and switches, hardening existing lines, and adding distributed generation facilities. The highlight of this study was the use of the more accurate AC model to represent the power flow which was seldom used in previous studies. A case study in the IEEE RTS-96 system tested the methodology. Bie et al. (2017) proposed a methodology which reconfigured the distribution system with distributed generator islanding after the hazards line earthquake happened. Two case studies have been done on an IEEE 33-bus system and a real Chinese urban distribution system; the results showed that the load shed of the system reduced significantly and improved the system's resilience. Lagos et al. (2019) utilized the optimization via simulation (OvS) solution approach to develop an optimal network investment model for improving the power system's resilience. The investment plan is optimized by Monte Carlo simulation for the performance of sets of investments which include adding new equipment and hardening substation against natural hazards like earthquakes. There are four phases for the simulation: threat characterization, vulnerability of systems components, system response, and restoration. A case study of an IEEE 12 bus network tested the model. Nazemi et al. (2019) proposed a linear-programming model to optimize the site and size of a battery energy storage system (BESS) to enhance resilience against earthquakes.

Modeling cascading outages is challenging due to the many mechanisms by which line outages can interact and propagate, including physical and cyber-physical interactions at different time and spatial scales as well as actions by human operators. We briefly review three approaches to credibly model cascading outages.

The first approach has been used by Vanzi (1996, 2000), Nuti et al. (2007), and Cavalieri et al. (2014) to model cascading related to earthquake damage. They focus on cascading consequences within substations and the propagation of short circuits to other substations. The cascading consequences within substations evaluate the reliability of classes of substation components considered as elements in series. The short-circuit propagation models earthquake damage that leads to a short circuit that is not isolated in the substation, which then leads to isolation of a connecting transmission line by a circuit breaker in another substation.

The second approach addresses cascading in general with no reference to earthquakes. There is a large literature that approximates a subset of the cascading outage mechanisms in a simulation (Baldick et al., 2008; Papic et al., 2011). These simulations are complicated and varied. Many of these simulations can produce credible cascades, and some progress has been made toward validating these simulations, so that samples of the simulated cascades have statistics that match the heavy-tailed distribution of cascade sizes observed in recorded blackouts (Bialek et al., 2016; Henneaux et al., 2018).

The third approach, as used in this article, is to sample directly from the statistics of observed cascades obtained by processing historical utility outage data. The recorded outages are grouped into cascades, and then into generations of outages within each cascade using the approach based on outage timing in the work of Dobson (2012). Then, the statistics for the number of outages in a cascade and the distance on the network can be extracted. Sampling from these statistics gives a probabilistic model of the spread of the cascading on the network consistent with the observed cascades. This type of modeling has been applied to quantify the resilience of transmission systems to storms and the effect of (photovoltaic) PV generation in the work by Kelly-Gorham et al. (2019, 2020).

Sampling the cascaded lines from an observed distributions is a simple and direct way to capture typical cascading behavior that, while approximate, produces realistic cascades. This approach includes all the varied mechanisms of general cascading. Moreover, we show in this article that, in contrast to simulation methods, when stratified sampling is used, the approach is computationally tractable when optimizing investments. Another approach to the statistical modeling of cascades spreading for resilience studies (Zhou et al., 2020) forms a Markovian influence graph from utility data, which describes how outages interact with each other.

A notable difference between our cascade modeling developed in the next section and that of Kelly-Gorham et al. (2020) is that we sample the number of cascaded outages from a branching process statistical model of the cascading with parameters estimated from the observed data, whereas Kelly-Gorham et al. (2020) sample directly from an empirical distribution of the total number of lines outaged. Kelly-Gorham et al. (2020) address the general resilience of the transmission system and there are many events available in the data to form an empirical distribution of the number of cascaded lines, whereas there are too few earthquakes to form a reliable empirical distribution of the number of cascaded lines for earthquakes.

The detailed outage data necessary for direct sampling of the outcomes of cascading is routinely collected by utilities, and in the United States, it is reported to national regulatory bodies. Thus, the detailed outage data needed are already available to utilities. However, since detailed outage data are sensitive and confidential, they are not usually accessible to researchers. In this article, we illustrate the method using publicly available data from a utility in the northern part of the Western United States' interconnection (Bonneville Power Administration (BPA), 2020).

Models

This analysis requires the integration of two models. The first model is a statistical model of cascade evolution given known physical damage to an electric power system. The second model is a stochastic program for investment planning where the individual scenarios are a combination of physical damage from a given earthquake and a realization of a cascade from that damage. This section discusses each of these models in turn.

Cascade model

When a transmission line is removed from service by automatic or manual controls, it is said to be outaged. Cascading of outages occurs when there is a dependent sequence of successive outages propagating through the electrical grid. When an earthquake occurs, the lines that are damaged or, more commonly that have damaged connections in substations

are outaged. After this initial damage, the disturbance to the system can cause other lines to outage in a cascade. The blackout associated with the damaged lines can become much more widespread due to the cascading. The cascading lines are out of service but not damaged, so that they can usually be restored within a day. However, the initial earthquake restoration can be greatly affected by the larger blackout caused by the cascading.

The electric power transmission system is modeled as a network with lines and nodes. In power systems, the nodes are called buses. The lines represent the transmission lines and the buses usually represent substations. The line reactance includes the series reactance of the transmission line together with the reactance of any transformers connected in series with the line. Each line joins two buses, known as the origin bus and the destination bus.

It has been shown that a branching process model parameterized by the measured cascade propagation can approximate the number of cascaded outages (Dobson, 2012). The amount of cascade propagation as the cascade progresses is measured from cascading data. Given the number of initial lines damaged in the earthquake, the branching process model calculates the probability distribution of the total number of lines outaged. Sampling from this distribution and subtracting the number of initial lines damaged in the earthquake gives the number of cascaded lines.

Given the number of cascaded lines, we need to locate them on the network. Cascades of line outages propagate not only locally to the neighboring lines but also to lines further away in the network. There are many different mechanisms by which line outages lead to further line outages, including redistribution of power flows in the network according to Kirchhoff's laws, various types of transients, automatic actions by the systems protecting the lines from overload, and actions by the human operators in control centers.

To capture the overall form of the cascade propagation we choose cascaded lines so that the probability distribution of their distances on the network match observed historical statistics of these distances based on Bonneville Power Administration data from the work of Dobson (2012) as shown in Figure 1. Here, the network distance is the number of "hops" between two lines. That is, the distance $\rho(L_1, L_2)$ between line L_1 and line L_2 is defined as the minimum number of buses in a network path joining the midpoint of L_1 to the midpoint of L_2. For example, the distance from L_1 to itself is 0, and the distance between two neighboring connected lines is 1.

To sample the cascaded lines according to the probability distribution of their distances on the network, let C be the set of initial damaged lines and k be the total number of cascaded lines. Choose an initially damaged line L_C from C randomly and sample a distance x from the distribution of the network distances between lines in a cascade. Next, randomly choose a line L_b from the network different than the lines in set C that satisfies $\rho(L_b, L_C) = x$. If there is no such a line, resample distance x or if this also fails, resample another L_C from C. Continue to sample cascaded lines in this way until there is a total of k cascaded lines.

Cascading phenomena require special sampling methods. Cascade size is inherently heavy-tailed, so that simple random sampling is ineffective in that it concentrates the sampling on the common small cascades, and has few or no samples of the rare large cascades that affect the risk the most. Stratified sampling in effect conditions the sampling on the number of cascaded outages so that samples are taken more uniformly over all cascade sizes and the sample variance is reduced (Owen, 2013). This prevents the underestimation or poor estimation of rare but high-risk cases with large numbers of cascaded outages.

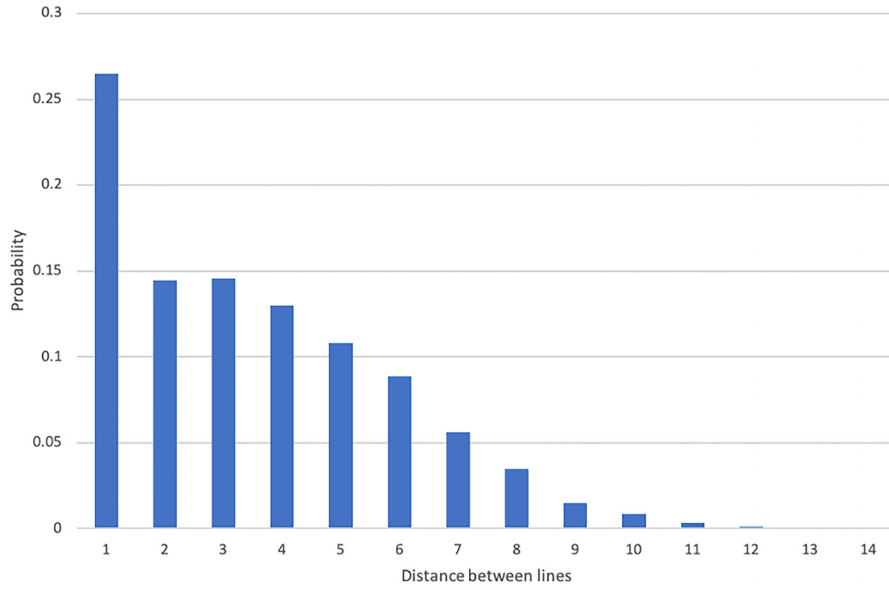

Figure 1. Probability of the network distance between lines in a cascade.

Stratified sampling is a simulation method that is more effective than plain Monte Carlo simulation. It is similar to importance sampling in that it changes the probability of sampled events with the goals of variance reduction and requiring fewer samples, but there are also differences in method detail as discussed in exploring Monte Carlo methods (Dunn and Shultis, 2011).

In stratified sampling, the population is partitioned into non-overlapping groups or strata, and samples are drawn from each of the strata. The strata are chosen so that the quantity being evaluated should not vary too much within each stratum. Then M random samples are chosen in each stratum.

In this study, the S strata $B_1,\ B_2,\ \ldots,\ B_S$ correspond to ranges of the total number of outaged lines N. Since the probability distribution of N is given by a formula (Dobson, 2012), it is straightforward to evaluate the probability of each stratum by Equation 1.

$$b_k = P[N \in B_k] = \sum_{r \in B_k} P[N = r] \tag{1}$$

Note that evaluating the probability of N with a formula is more accurate than sampling from the distribution of N. The goal of the sampling is to estimate the expectation of the cost (noted as *Cost*) of the restoration after the earthquake. The expected cost for each stratum k is estimated with M samples $n_1,\ n_2,\ \ldots,\ n_m$ by Equation 2.

$$E[Cost|N \in B_k] = \frac{1}{M} \sum_{m=1,\ n_m \in B_k}^{M} Cost(n_m) \tag{2}$$

The expectation of the cost of the restoration after the earthquake is estimated by conditioning on the stratums by Equation 3.

$$E[Cost] = \sum_{k=1}^{S} b_k E[Cost|N \in B_k] = \sum_{k=1}^{S} b_k \frac{1}{M} \sum_{m=1,\ n_m \in B_k}^{M} Cost(n_m) \tag{3}$$

Investment planning model

We use the investment planning model developed in the work of Romero et al. (2013), which is a two-stage stochastic program. Stochastic programs are optimization models that include uncertainty, and that uncertainty is characterized by a set of scenarios, each with a specific occurrence probability (Birge and Louveaux, 2011). In this case, each scenario specifies the physical damage from an earthquake event as well as a specific realization of a cascade from that damage.

In the first stage, the investments in the electric power system are made. These investments focus on expanding transmission lines and generation capacity at existing plants. Lines can be expanded in increments of 25% of the original capacity and are limited to a doubling of that original capacity. Similarly, generators can be expanded in increments of 20% of the original capacity of that unit to a maximum of 40% of its original capacity. The second stage captures the restoration process as well as the optimized use of on hand spare components. For the second stage, for each scenario, the load shed and generation cost over the restoration process are computed. The objective of the stochastic program is to maximize the performance of the electric power system during the restoration process, where the performance of the power system is measured as the negative of the sum of the power generation costs and the load shed costs.

For each earthquake event, the damage to each component is estimated based on the HAZUS methodology (Federal Emergency Management Agency (FEMA), 2020). There are five damage states for the components of an electric power system: none, slight, moderate, extensive, and complete. We focus on line and substation damage only. For transmission lines, we only model extensive and complete damage, extensive damage is defined by the failure of 50% of all circuits and corresponds to a damage ratio of 60% of the total cost. The complete damage of transmission lines is defined by the failure of 80% of all circuits and corresponds to a damage ratio of 100% of the total cost. For substation, we only focus on damage to transformers and only model moderate, extensive and complete damage, because the transformers are the main factor of the restoration process of substations due to their long repairing time (Romero et al., 2013). The moderate damage for substation corresponds to a repair cost of 11% of substation cost and is defined as the failure of 40% of disconnect switches, circuit breakers, and current transformer. The extensive damage for substation corresponds to a repair cost of 55% of substation cost and is defined as the failure of 70% of disconnect switches, circuit breakers, and current transformer. The complete damage for substation corresponds to a repair cost of 100% of substation cost and is defined as the failure of all of disconnect switches, circuit breakers, and current transformer (FEMA, 2020).

Furthermore, HAZUS also provides mean restoration times for lines and substations, which are used to define the duration of the different parts of the restoration process (FEMA, 2020). Consistent with this reference, we assume that to repair a line with extensive damage is 3 days and to repair a line with complete damage is 7 days. For substation,

the time to repair for moderate damage is 3 days, for extensive damage is 7 days, and for complete damage is 30 days. Similar to the study done by Romero et al. (2013), we assume that a substation with complete damage that has low-voltage transformers is back in service within a month and that substations in a state of complete damage with medium and high-voltage transformers are back in service within 6 months. Therefore, at the end of the sixth month after the earthquake, the system is back to normal.

As a result, the restoration process is assumed to be 6 months in duration and is organized as consecutive time periods. The time periods are shorter at the beginning of the restoration process and are longer at the end because some components are quicker to fix than others. The first nine time periods are 8 h in length. The tenth time period extends from the beginning of day 4 to the end of day 7. The 11th time period concludes at the end of the first month after the earthquake and the 12th time period extends from the end of the first month after the earthquake to the end of the sixth month after the earthquake.

We assume that for each period from the first time period to the ninth time period, a random number of cascaded lines are fixed, and by the end of ninth time period, all cascaded lines are in service. For the repair of the physical damage, by the end of ninth time period, all transmission lines with extensive damage and substations with moderate damage are repaired; by the end of tenth time period, the transmission lines with complete damage and the substation with extensive damage are repaired; by the end of 11th time period, the substations with both complete damage and loss of low-voltage transformers are be repaired; and by the end of 12th period, the substations with complete damage and the loss of medium and large voltage transformers are repaired.

The objective function is given in Equation 4. The objective is to minimize the expected generation and load shed costs over the 12 periods.

$$\min \sum_{n=1}^{N} pr(n) \sum_{k=1}^{K} w_k \left(\sum_{i \in B} c^B U_i^{nk} + \sum_{g \in G} c_g^G G_g^{nk} \right) \tag{4}$$

where n is the nth scenario, $pr(n)$ is the probability of the nth scenario and equals $S(n)b_n$ $1/M_n$, where $S(n)$ is the probability of the earthquake that leads to the physical damages in the nth scenario, b_n is the probability of the strata that contains the total number of failed lines in the nth scenario, and M_n is the number of scenarios in this strata. Also, let N be the number of total scenarios, k be the kth time period, and K be the number of time periods, B be the collection of buses, i be the bus number, c^B be the load shed cost per unit of load shed, and U_i^{nk} be the load shed for bus i in the kth time period in scenario n. Finally, let G be the collection of generators, g be an index over the generators g, and c_g^G be the cost of generation per unit for generator g. G_g^{nk} is the generation variable for generator g in the kth time period in scenario n. Notice that by inserting a weight indexed by time period w_k inside the second summation sign in Equation 4, we can assign different importance to load shed across periods.

The model is constrained by power flow constraints, budget constraints, flow conservation constraints, demand constraints, and capacity constraints. The power flow constraints for each time period are given in Equations 5 to 7, where θ_i^{nk} is the phase angle for bus i in the kth time period in scenario n, θ_j^{nk} is the phase angle for bus j in the kth time period in scenario n, Λ_{ij}^{nk} is the damage state of line (i, j) in the kth time period in scenario n, $\Delta_{s_i}^{nk}$ is the damage state for substation s_i in the kth time period in scenario n, $\Delta_{s_j}^{nk}$ is the damage

state of substation s_j in the kth time period in scenario n, ρ represents 25% of the original capacity of line (i, j), w_{ij} is the number of increments added to the capacity of line (i, j), X_{ij} is the reactance of line (i, j), P_{ij}^{nk} is the real power flow in line (i, j) in the kth time period in scenario n, and T_{ij} is an indicator parameter that represents whether a spare transformer for line (i, j) can be obtained quickly.

$$(\theta_i^{nk} - \theta_j^{nk})(1 - \Lambda_{ij}^{nk})(1 - \Delta_{s_i}^{nk})(1 - \Delta_{s_j}^{nk})\left(1 + \rho w_{ij}\right) = X_{ij}P_{ij}^{nk}, \forall(i,j),\ \forall n,\ k \leqslant 10 \tag{5}$$

$$(\theta_i^{nk} - \theta_j^{nk})(1 - \Delta_{s_i}^{nk})(1 - \Delta_{s_j}^{nk})\left(1 + \rho w_{ij}\right) = X_{ij}P_{ij}^{nk},\ \forall(i,j),\ \forall n,\ k = 11 \tag{6}$$

$$(\theta_i^{nk} - \theta_j^{nk})(1 - \Delta_{s_i}^{nk}\left(1 - T_{ij}\right))\left(1 + \rho w_{ij}\right) = X_{ij}P_{ij}^{nk},\ \forall(i,j),\ \forall n,\ k = 12 \tag{7}$$

The budget constraint is given in Equation 8, where Π is the collection of all lines, h_{ij} is the cost to add a capacity increment to line (i, j), o_g is the cost to add a capacity increment to generator g, z_g is the number of increments add to the capacity of generator g, and M^C is the budget.

$$\sum_{(i,j)\in\Pi} h_{ij}w_{ij} + \sum_{g\in G} o_g z_g \leqslant M^C \tag{8}$$

The flow conservation constraint is given in Equation 9, where D_i is the demand of bus i, $I(i)$ is the set of generators connected to bus i, $\delta^+(i)$ is the set of lines such that the origin bus is i, and $\delta^-(i)$ is the set of lines such that the destination bus is i.

$$\sum_{g\in I(i)} G_g^{nk} - \sum_{(i,j)\in\delta^+(i)} P_{ij}^{nk} + \sum_{(i,j)\in\delta^-(i)} P_{ij}^{nk} = D_i - U_i^{nk},\ \forall n,\ k, i \tag{9}$$

The demand and capacity constraints are shown in Equations 10 to 14, where G_g^c is the capacity of generator g, P_{ij}^c is the capacity of line (i, j), and represents 20% of the original capacity of generator g.

$$0 \leqslant U_i^{nk} \leqslant D_i,\ \forall n,\ k, i \tag{10}$$

$$0 \leqslant G_g^{nk} \leqslant G_g^c(1 + \mu z_g),\ \forall n,\ k, g \tag{11}$$

$$\left|P_{ij}^{nk}\right| \leqslant P_{ij}^c(1 - \Lambda_{ij}^{nk})(1 - \Delta_{s_i}^{nk})(1 - \Delta_{s_j}^{nk})\left(1 + \rho w_{ij}\right), \forall(i,j),\ \forall n,\ k \leqslant 10 \tag{12}$$

$$\left|P_{ij}^{nk}\right| \leqslant P_{ij}^c(1 - \Delta_{s_i}^{nk})(1 - \Delta_{s_j}^{nk})\left(1 + \rho w_{ij}\right), \forall(i,j),\ \forall n,\ k = 11 \tag{13}$$

$$\left|P_{ij}^{nk}\right| \leqslant P_{ij}^c(1 - \Delta_{s_i}^{nk}(1 - T_{ij}))(1 + \rho w_{ij}), \forall(i,j),\ \forall n,\ k = 12 \tag{14}$$

Case study

Scenario definition

As mentioned previously, we focus on mitigating the impact of the New Madrid Seismic Zone on the Eastern Interconnection. The representation of Eastern Interconnection used in this study was developed in 1998 by the Multi-Area Modeling Working Group which

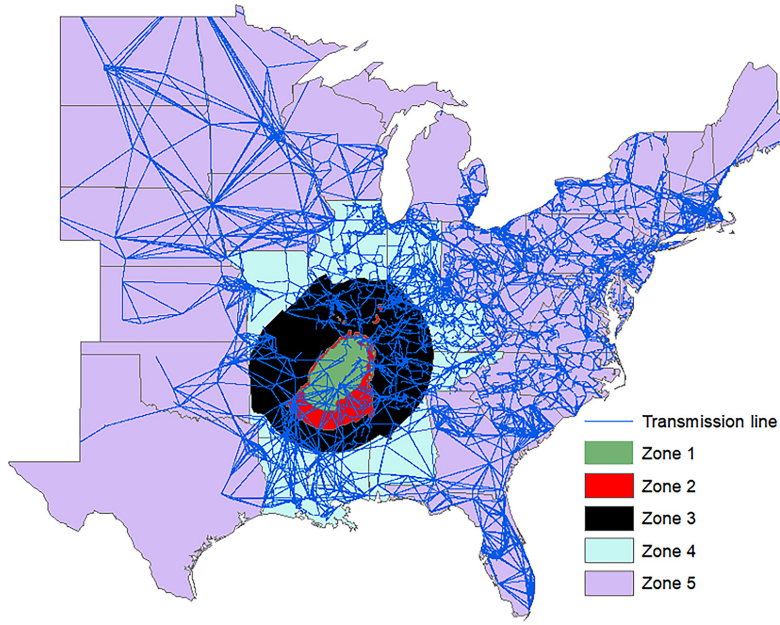

Figure 2. Division of the study area.

belongs to the Eastern Interconnection Reliability Assessment Group (ERAG, 1998). In this representation, the network has 23,416 transmission lines and transformers, 14,957 buses, and 2765 substations. The power demands reflect a prediction of the summer of 2003 and all the costs in this study are estimated in 2002 USD. We effectively extend the analysis in the work of Romero et al. (2013), which focused on the Eastern Interconnection and the New Madrid Seismic Zone, to include the impacts of cascading and investigating the impacts of more highly prioritizing the load shed in the first 3 days after the earthquake.

The study area is divided into five zones based on the shake map of New Madrid Seismic Zone and those zones are shown in Figure 2 (Central United States Earthquake Consortium (CUSEC), 2014). This shake map is created by utilizing the modified Mercalli intensities (MMIs) data for the large earthquakes near New Madrid, Missouri (Bakun et al., 2002). Zone 1 is the area with the MMI level between 7.0 and 9.3, which is the highest risk area. Zone 2 is the area with MMI level between 6.0 and 6.9. Zone 3 is the area with MMI level between 5.0 and 5.9. Zone 4 includes the states which surround Zone 3 and exclude Zone 3. Zone 5 is the entire study area excluding Zones 1–4.

To model the seismic risk from New Madrid Seismic Zone, eight earthquake scenarios are selected by the mathematical optimization method developed by Vaziri et al. (2012). Given the candidate set of earthquake events from US Geological Survey (USGS, 2008a), and 81 control points in the New Madrid Seismic Zone also used by Romero et al. (2013), annual occurrence probabilities are identified for to each scenario that minimize the discrepancy with seismic behavior as represented in the exceedance curves for peak ground acceleration (PGA) at control points throughout the New Madrid Seismic Zone. The candidate set of earthquakes, of which the eight are selected, stem from 433 historical events in the

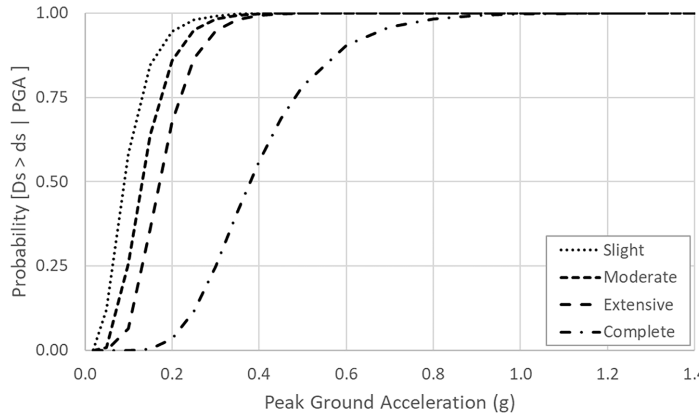

Figure 3. Fragility curves for high-voltage substation with unanchored/standard component.

New Madrid Seismic Zone (USGS, 2008a) and 20 synthetic earthquake scenarios from USGS (2008b) which correspond to four magnitude (7.3, 7.5, 7.7, and 8) ruptures in five branches of the New Madrid fault system described in the work of Petersen et al. (2008). For each event, we use Petersen et al. (2008), Atkinson and Boore (1995, 2006), Frankel et al. (1996), Johnston (1996), Toro et al. (1997), Campbell (2003), Tavakoli and Pezeshk (2005), and Silva et al. (2002) to compute ground motion at each control point.

In terms of estimating the probability of each component suffers specific levels of damage under each scenario, the fragility curves from HAZUS are used (FEMA, 2020). Given the PGA value at the location of the component of the power system, the fragility curves or damage function can evaluate the probability of that component reaching or exceeding different damage states (FEMA, 2020). A sample fragility curve from HAZUS is shown in Figure 3, which is the fragility curve for high-voltage substation with unanchored/standard components (FEMA, 2020).

Similar to the study conducted by Romero et al. (2013), the probability that each component suffers the different levels of damages under each earthquake scenario is modeled as a set of consequence scenarios. We applied the optimization method developed by Gearhart et al. (2014) to generate the consequence scenarios for each earthquake scenario and their adjusted occurrence probabilities. The goal of this method is to find consequence scenarios and their corresponding probabilities such that minimizing the discrepancy between the implied vulnerabilities of each component and their "true" vulnerabilities (Gearhart et al., 2014) while preserving the spatial correlation in that damage.

After investigating the eight earthquake scenarios that represent the seismic risk from New Madrid Seismic Zone, only two of these eight scenarios can cause any significant damage to the electric power system. Each of these two earthquake scenarios is used to generate six consequence scenarios, each of which identifies the damage state for each component (Gearhart et al., 2014). These damage scenarios are created in a manner as to preserve the spatial correlation in damage based on the underlying spatial correlation in ground shaking.

Table 1. Twelve earthquake damage scenarios

Earthquake scenario	Probability	Extensive line damage	Complete line damage	Moderate substation damage	Extensive substation damage	Complete substation damage
1	0.000160	5	24	18	8	15
2	0.000200	5	25	23	19	8
3	0.000080	15	24	68	24	10
4	0.000180	4	25	13	14	10
5	0.000240	6	24	12	16	9
6	0.000140	6	22	26	22	12
7	0.000126	27	11	35	16	14
8	0.000396	28	14	4	13	11
9	0.000288	30	13	17	12	12
10	0.000342	28	13	6	7	19
11	0.000432	24	14	5	13	13
12	0.000216	28	26	25	10	13

Across all six damage scenarios for an earthquake scenario and for a specific component, the probability distribution for the damage state approximates the distribution for damage given the PGA at that location in the assumed earthquake based on the fragility curves in HAZUS (FEMA, 2020). Table 1 gives statistics for the 12 damage scenarios. For further information, Romero et al. (2013) describe how the earthquake and damage scenarios were developed.

Given an initial number of damaged lines, the distribution of the total number of lines that are not functional after the earthquake due to further cascading is determined through a branching process model (Dobson, 2012) and the cascade spreading model described in cascade model section with the following assumptions: (1) 40 cascades are estimated for each damage scenario resulting in 480 scenarios in the stochastic program; (2) for each damage scenario, 20 strata (where each stratum is defined as a range in the number of lines cascaded) are used to create the 40 realizations for the number of lines cascaded; (3) sampling within each strata is uniform and two realizations from each bin are drawn randomly for each physical damage scenario; (4) for earthquake damage scenarios 1–11 in Table 1, the strata are defined as 50 minus the number physically damaged for the first strata and the remainder are defined in blocks of 50; (5) for earthquake damage scenario 12, the first and second strata are from 54 to 80, and 81–100 total lines out after the event and the remainder in blocks of 50; and (6) the maximum number lines damaged and cascaded in a scenario is 1000. Theoretically, the maximum number of outage lines is the total number of lines in the system 23,416; however, by looking at the distribution of total number of outage lines for each of the damaged scenarios in Table 1, a maximum of 1000 tripped lines captures 99.9% of the empirically estimated distribution for outage size.

The cascade model described in cascade model section is used to locate the cascade lines in the power system for all 480 scenarios for use in the stochastic program. Figure 4 illustrates four scenarios for the stochastic program created using damage scenario 1 in Table 1. Scenario 1 identifies 29 lines as damaged. In the cascade illustrated in Figure 4a, an additional 211 lines describe the associated cascade. The largest of the cascades stemming from the physical damage is given in Figure 4d with 955 lines in the cascade. Notice that the actual damage is located in a very confined region (Mississippi and Kansas), but the cascaded lines can be quite removed from the damaged portions of the network. In

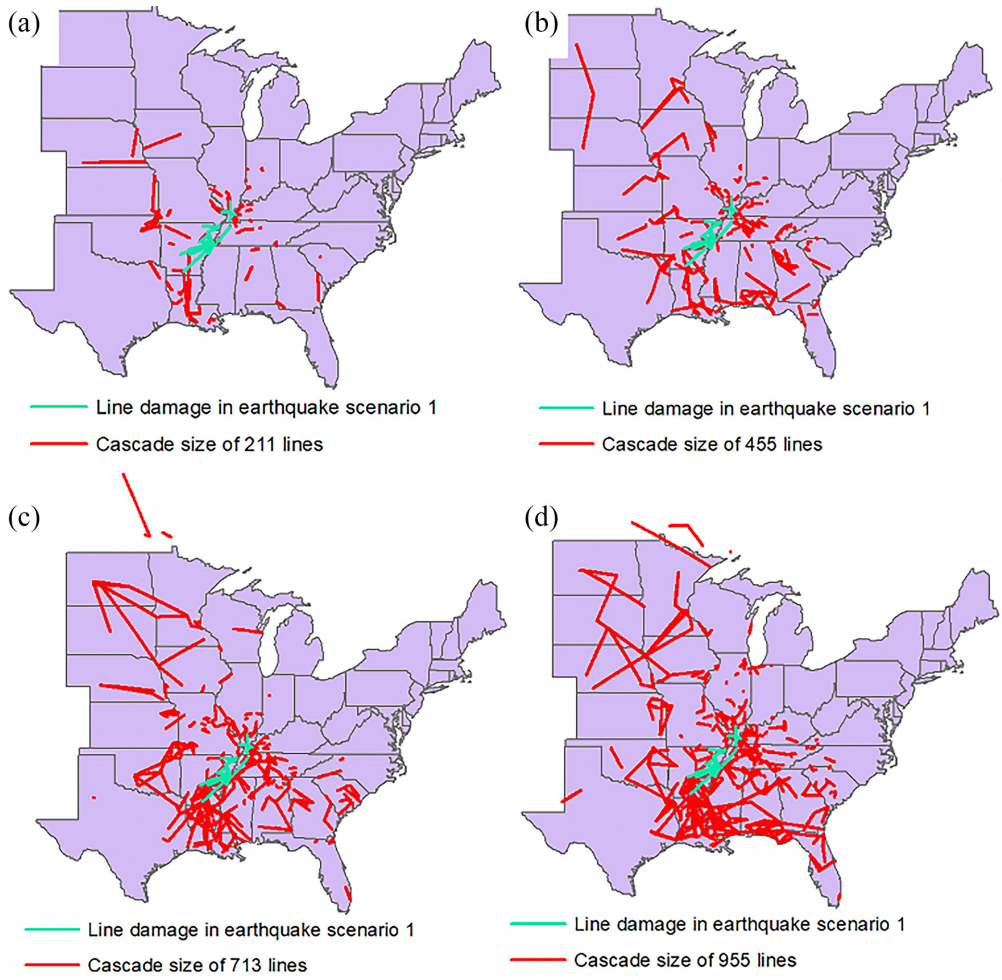

Figure 4. Four illustrative cascades size of (a) 211, (b) 455, (c) 713, and (d) 955 stemming from damage scenario 1 in Table 1.

this scenario, the cascade lines extend into Canada (as they also do in the scenarios illustrated in Figure 4c).

Experiments

As mentioned previously, this computational study is focused on two questions: (1) whether inclusion of the cascades impacts the recommended investments to control earthquake risk and (2) the impact on the investment plan of focusing more heavily on outages in the first 3 days after the earthquake instead of more evenly over the restoration process. The first question is investigated by comparing the investment plans using all 480 scenarios (40 cascade scenarios stemming from each damage scenario) and one with only 12 scenarios each of which is identified in Table 1. The second question is investigated using the stochastic program with all 480 scenarios and comparing the investment plans when w_k are equal for all 12 time periods and a second experiment where w_k is one for the

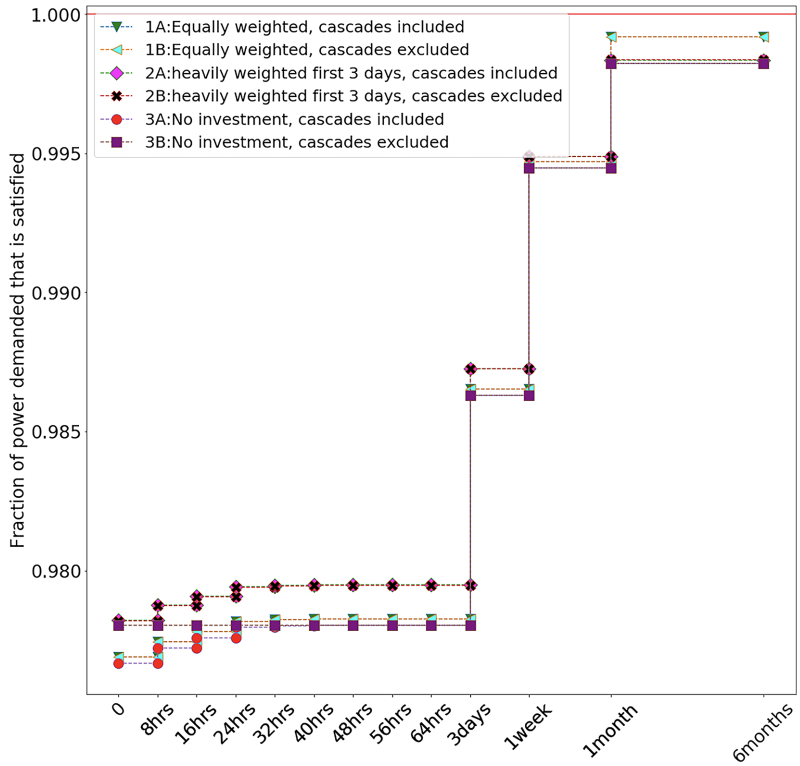

Figure 5. Restoration curves for the six different experiments for the entire study region (US$100 million investment budget where applicable).

first nine time periods and is a very small value for the remainder of the time periods (i.e. $w_1 = w_2 = \ldots = w_9 = 1$ *and* $w_{10} = w_{11} = w_{12} = \varepsilon$ *where* $\varepsilon \ll 1$). Finally, we restrict the investments in all experiments to the four zones in Figure 2, which are the ten states: Indiana, Kentucky, Tennessee, Georgia, Alabama, Mississippi, Louisiana, Arkansas, Missouri, and Illinois.

Figure 5 gives the average load shed for the four experiments described above which are labeled as follows: (1A) load shed in all periods are equally weighted and cascades are considered in investment model, (1B) load shed in all periods are equally weighted and cascades are not considered in investment model, (2A) load shed in the first 3 days are the priority and cascades are considered in investment model; and (2B) load shed in the first three periods are the priority and cascades are not considered in investment model. For comparison, two more cases labeled 3A and 3B are as follows: (3A) includes cascades but no investment and (3B) includes no cascades and no investment. Experiments 3A and 3B assume that $w_{ij} = 0$, $\forall(i,j)$ and $z_g = 0$, g. For experiments 1–4, the investment budget is US$100 million.

The average restoration curves for the entire study area and the region comprising Zones 1 and 2 for all six experiments are given in Figures 5 and 6 when the investment budget is US$100 million. For experiments with scenarios, we average the load shed in each period using the scenario probabilities. For experiments 1B and 2B, where no

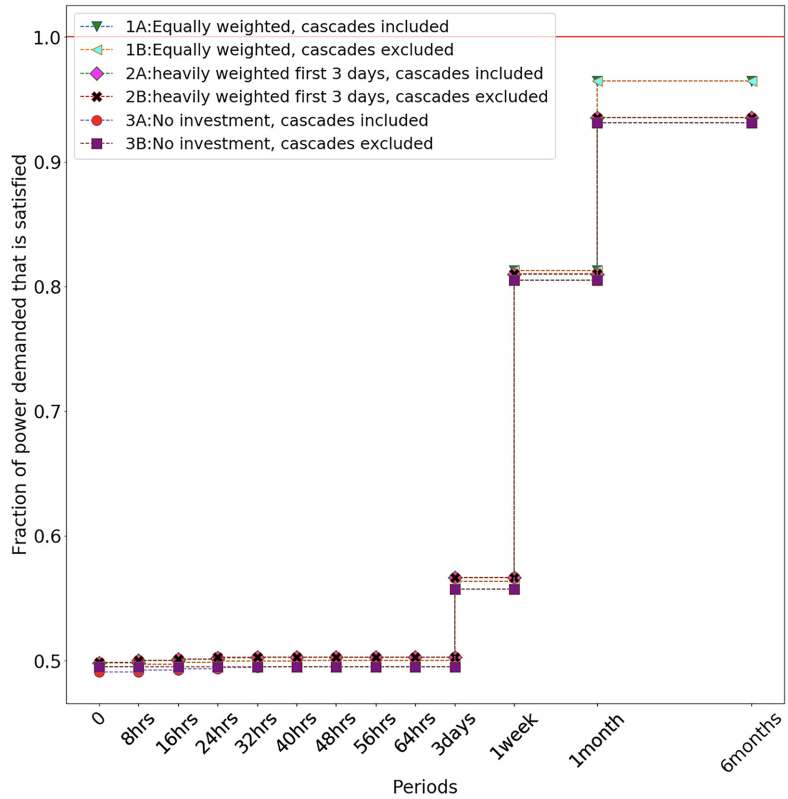

Figure 6. Restoration curves for six different scenarios in Zones 1 and 2.

cascades are considered in the stochastic program, the restoration curve is computed after the investment plan is identified assuming those cascades occur, because while they are not considered in the optimization when those investments are made, their performance when an earthquake occurs is impacted by the occurrence of cascades.

First, notice that when no investment is made and cascades are not considered (experiment 3B) the average restoration curve is flat for the first 3 days. This is because effectively nothing that has been damaged can be repaired that quickly. Lines with extensive damage are assumed to take more than 3 days to restore. Of course, the cascades will make the load shed worse in the first 3 days which is illustrated in experiment 3A. The key insight is that if cascades are not considered, we are likely to overestimate the performance of the electric power system after the earthquake. Second, notice the impact of the investment plans (with US$100 million available for investment) are the same whether or not they were developed using cascades (in these experiments). This same behavior is observed when the focus is on the first 3 days or the entire restoration process. This implies that we can simplify our investment optimization by not including cascades in the scenarios thereby drastically reducing the number of scenarios in the optimization but, afterwards, estimating the performance of the electric power system after investment under the earthquake threat with cascades. This has substantial computational benefits. Finally, when the emphasis is on the first 3 days, the load shed is significantly lower in the first 3 days (which can substantially help the restoration of other infrastructure as well as support

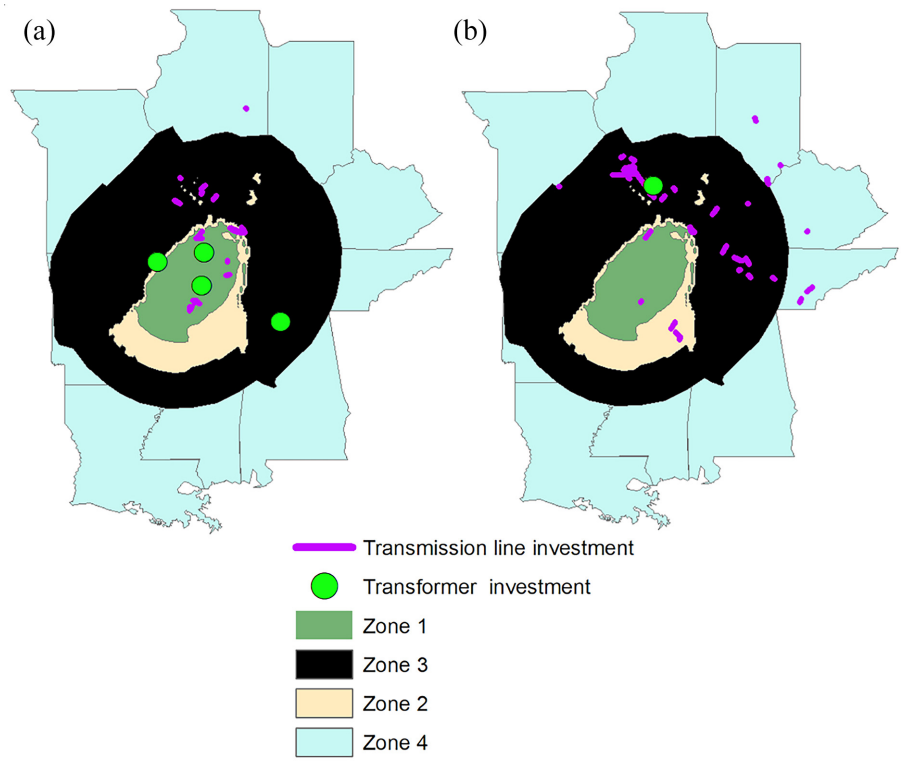

Figure 7. Location of line investment in four experiments (a) experiments 1A/1B and (b) experiments 2A/2B.

rescue operations). In fact, the load shed is lower through the first month. However, in the last 5 months, the load shed is worse.

The recommended investments for experiments 1A and 1B are exactly the same; that is, the same 43 components receive investments under both plans; 39 of them are transmission lines and four of them are transformers. The locations of these investments are shown in Figure 7a; as expected, most of these investments are concentrated in Zones 1 and 2. As for experiments 2A and 2B, again, the investment plans are identical. Sixty-seven components receive investments in experiments 2A and 2B. Sixty-six components are transmission lines and one component is a transformer. The locations of the investments in experiments 2A and 2B are shown in Figure 7b.

Notice that when we focus on the load shed in the first 3 days, the locations of the investments are more geographically distributed with most of them occurring in Zone 3. One potential explanation for this "spread out" in investments in experiments 2A and 2B is, when the emphasis is on the early periods of the restoration process, those areas with larger populations are protected with additional investment in contrast to less densely populated areas. Figure 8a and b shows the population by county (United States Census Bureau, 2003) and the location of the investments for experiments 1A/1B and 2A/2B, respectively. Notice that the locations of the investments in experiments 2A/2B are in and near the cities of St Louis, Nashville, and Memphis. The investments within these counties

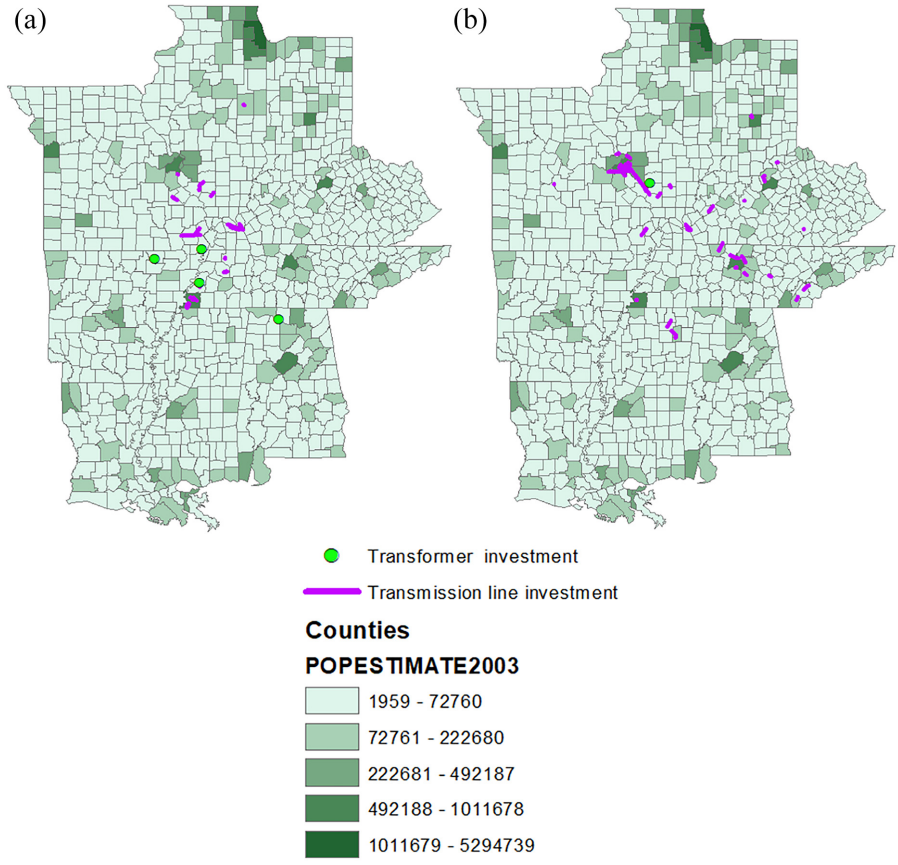

Figure 8. County population map and investment in 2003 (a) experiments 1A and 1B and (b) experiments 2A and 2B.

account for US$56.9 of the US$100 million invested in experiments 2A/2B but only account for US$28.5 of the US$100 million invested in experiments 1A/1B. This results in a substantially improved restoration profile for those counties in the first 3 days as illustrated in Figure 9 under experiments 2A/2B in contrast to experiments 1A/1B.

Figure 10 gives boxplots of the expected total load shed costs over the 6-month period across the entire study region (Zones 1–5) for each of five budget levels (US$100, US$300, US$500, US$700, and US$900 million). Notice that more scenarios suffer significant higher load shed costs under experiments 2A/2B than over experiments 1A/1B at each funding level because the mean load shed is higher, and the high end of the tail is longer. However, based on Figure 11, the load shed costs are lower in the first month under experiments 2A/2B than experiments 1A/1B. Across both Figures 10 and 11, it is also clear that considering cascades in the optimization has virtually no effect on the benefits derived from the plans developed.

Each of the investment plans created under experiments 1A/1B at all budget levels include the same investments in four specific transmission lines, and these lines are illustrated in Figure 12. The combined cost for these four investments is US$24.4 million.

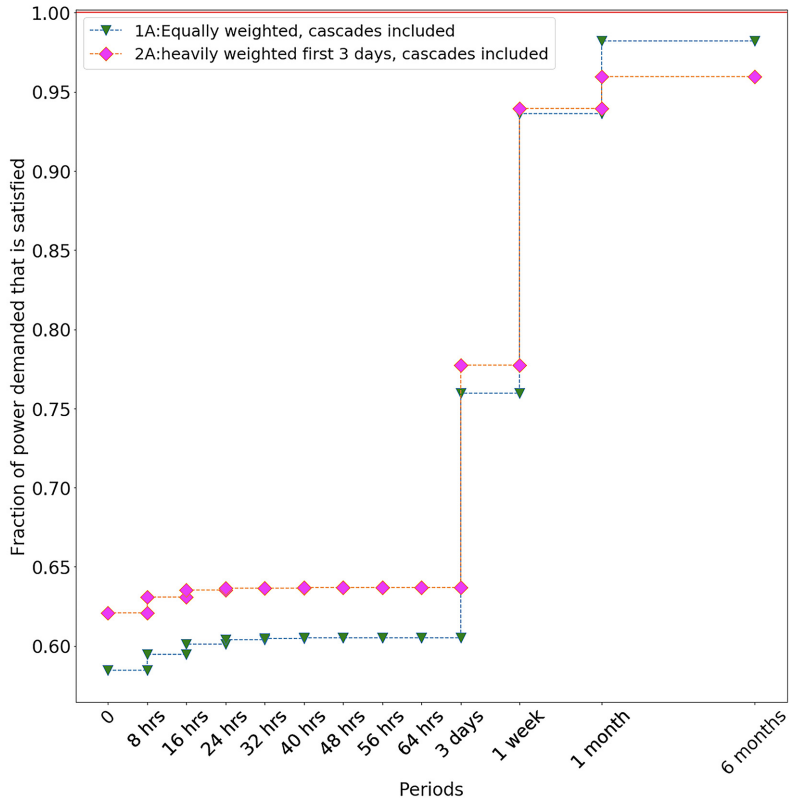

Figure 9. Restoration curves for areas of St Louis, Nashville, and Memphis.

Figure 13 gives a box plot of the impact of these four investments only and a comparison with the load shed costs with no investments and an investment of US$100 million. Notice that these four lines, which cost about 25% of the US$100 million budget, reduce median load shed by about US$524 million, whereas the full US$100 million budget reduces median load shed by about US$1400 million; that is, these four investments comprise about 37% of the median benefit of the US$100 million budget. Similarly, for experiments 2A/2B, nine transmission lines receive the same investments at all budget levels and those lines are illustrated in Figure 14. The combined cost for these nine investments is US$11.2 million and Figure 15 gives a box plot of the impact of these nine investments on load shed costs only as well as a comparison of those investments with no investments and an investment of US$100 million under experiment 2A. The median load shed cost is reduced by about US$88 million under this nine-line investment which is about 14% of the median benefit of the US$100 million investment budget.

Table 2 gives the common investments across all four experiments (1A/1B/2A/2B) at each budget level. The level of common investments for budgets of US$100 and US$500 is quite small, though the value of those investments, at least for a budget of US$500 million is relatively large (in comparison with the cost of the investments). For budgets of US$300, US$700, and US$900 million, the costs of the common investments are about 10% of the total invested whereas for a budget of US$700 million, the median benefits (across the 480

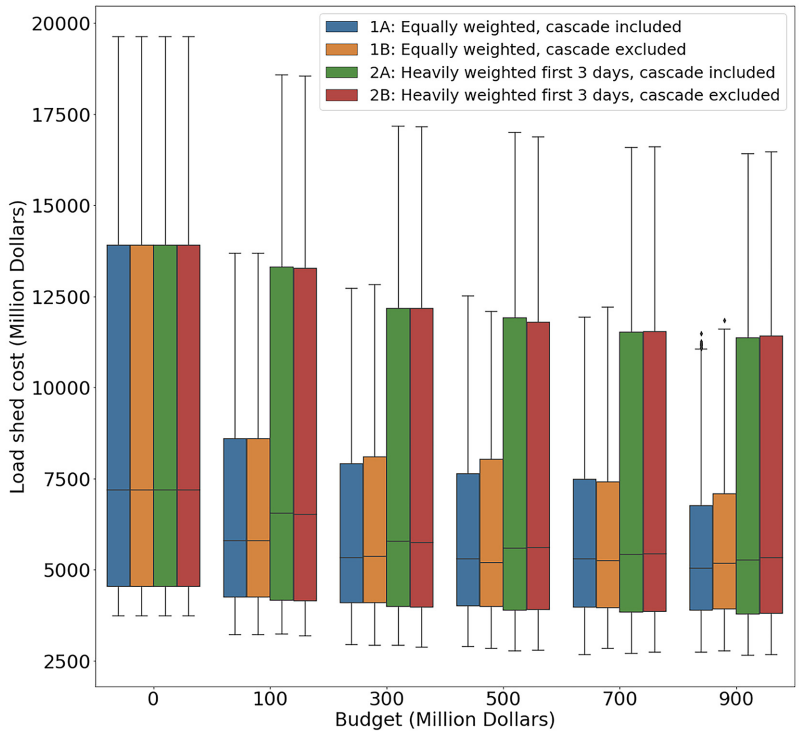

Figure 10. Distribution of load shed cost by budget across the 6-month restoration process.

scenarios) are on the order of 1.5 to twice the costs and for a budget of US$900 million, the median benefits are more than twice the costs.

Conclusion

This article addresses two questions about capacity expansion investment to increase the resilience of electric power transmission systems to earthquakes: (1) What is the effect of including cascading in the investment optimization model? and (2) How does the investment change when focusing more heavily on outages in the first 3 days after the earthquake rather than more evenly over the restoration process? We show how to model the more widespread blackout beyond the initial physical damage with statistical models of the size and spread of the cascading outages that are driven by observed blackout data. And we demonstrate computational tractability on a very large network model (14,957 buses) of an interconnection by deploying these statistical models of cascading with stratified sampling.

We focus on a case study of the Eastern Interconnect using the investment model developed by Romero et al. (2013) integrated with a statistical model of cascades. Essentially, equivalent investment plans are identified whether or not cascades are included in the investment planning model, which greatly simplifies the resultant optimization. However, cascades do significantly initially impair grid performance, and therefore, it is necessary to consider cascading after the earthquake to avoid underestimating the load shed in the early periods of the recovery. While not quantified here, the more widespread blackout

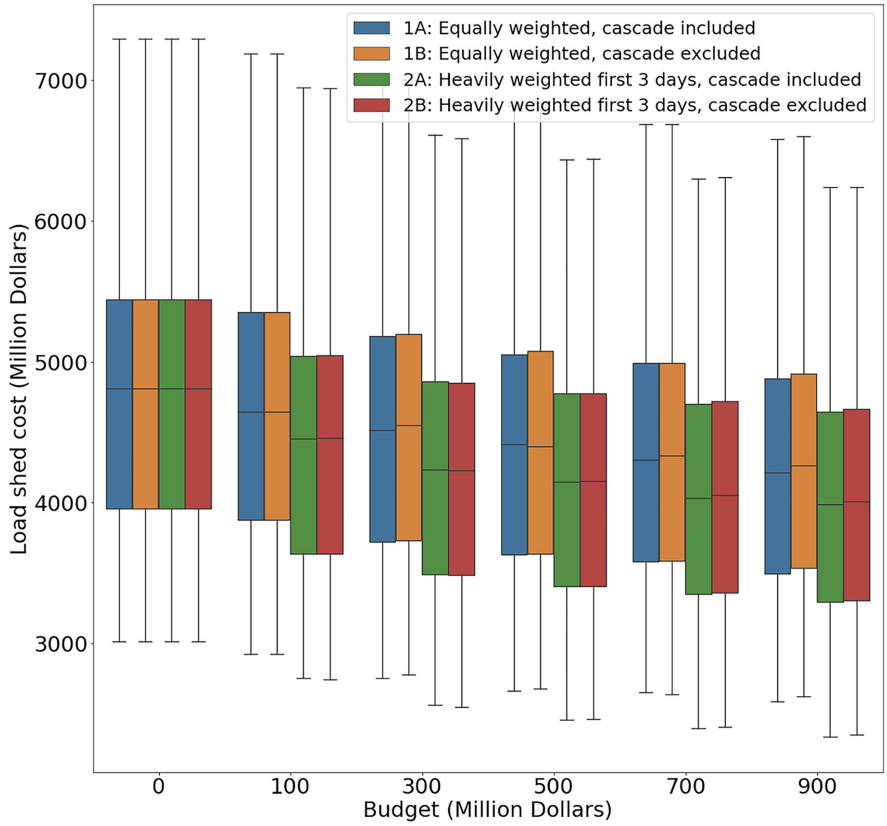

Figure 11. Distribution of load shed cost during the first month by budget.

due to cascading does affect the immediate emergency recovery and could lead to a greater loss of life.

We do find that when significantly more weight is placed on outages in the first 3 days, the load shed is not only significantly lower in the first 3 days, but also lower through the first month. However, in the last 5 months, the load shed is measurably worse. Furthermore, when focusing more heavily on outages in the first 3 days after the earthquake, areas with higher population tend to receive more investments than areas with lower population. In this study, these areas are near the cities of St Louis, Nashville, and Memphis. It is also worth noting that there do appear to be some critical lines that benefit from investment under multiple budget assumptions. For example, when all outages are equally weighted, four transmission lines are recommended for investment regardless of budget level. In the US$100 million investment case, investment in these lines costs only US$24.4 million, but comprises about 37% of the benefit.

Future work is needed in at least five areas. First, the method to select the earthquake scenarios and the annual probability of occurrence for each does not explicitly preserve spatial correlation in ground shaking. Empirically, it is found to be close because it identified a subset of events which each produce spatially correlated ground shaking and collectively reproduce exceedance curves that are spatially distributed. However, a method could

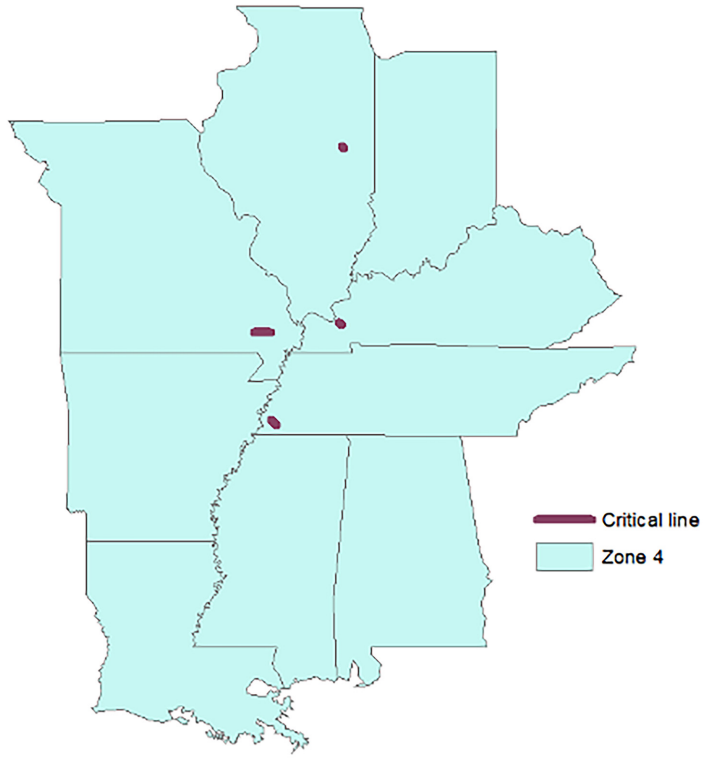

Figure 12. Persistent transmission line investments across all budgets for experiments 1A/1B.

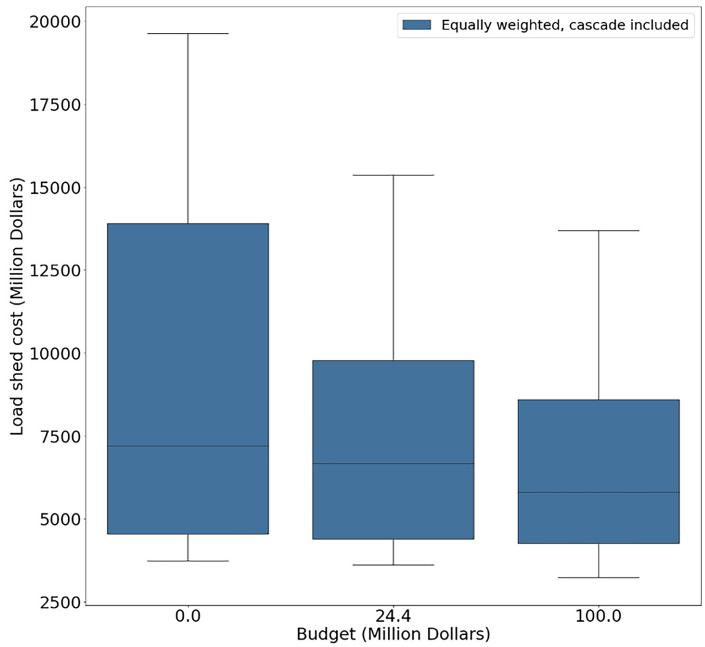

Figure 13. Load shed cost with identified critical components and comparison to related budgets (1A/1B).

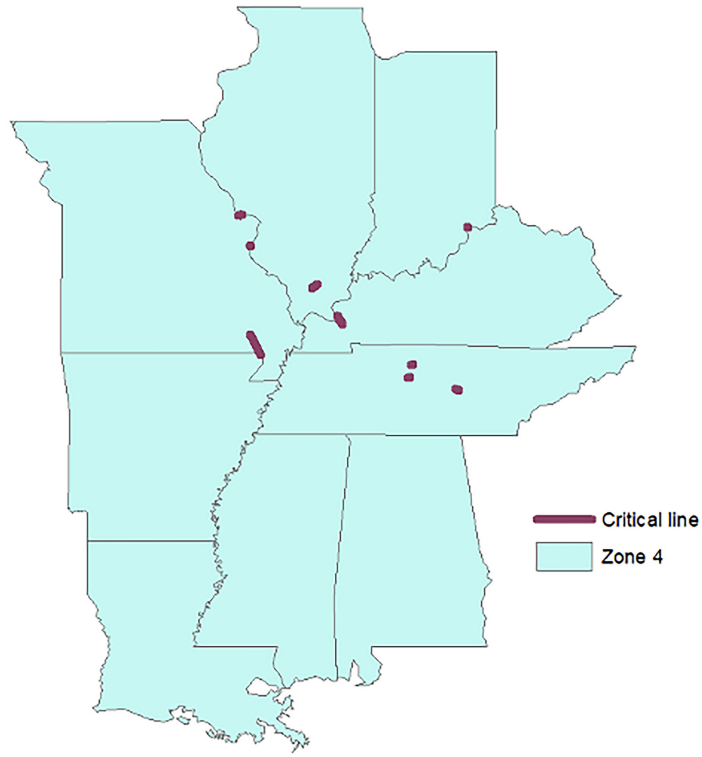

Figure 14. Persistent transmission line investments across all budgets for experiments 2A/2B.

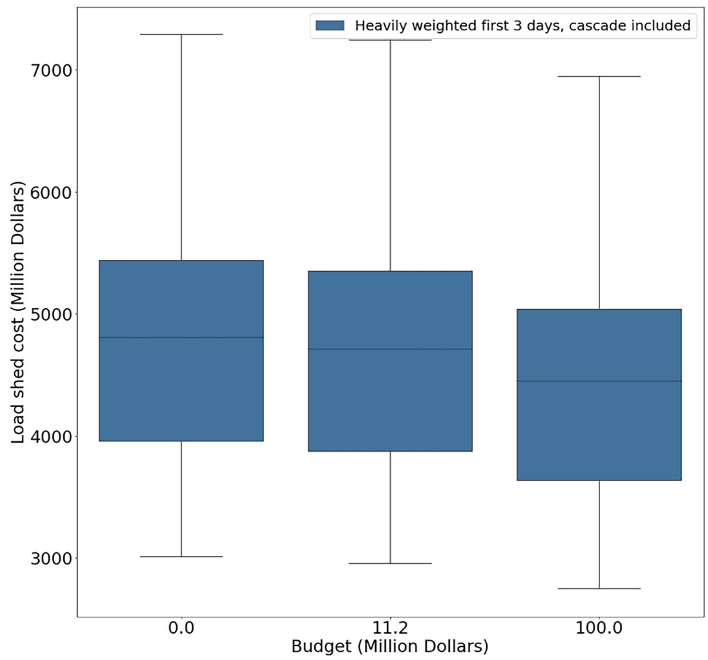

Figure 15. Load shed cost with identified critical components and comparison to related budgets (2A/2B).

Table 2. Common investments for experiments 1A/1B/2A/2B at each budget level

Budget level (million US$)	Number of common investment	Cost (percentage of the budget) (%)	Percentage of the median benefit of the full budget investment
100	2	0.78	1A: 1.27%, 1B: 1.27%, 2A: 2.73%, 2B: 2.63%
300	7	9.44	1A: 9.29%, 1B: 9.51%, 2A: 12.17%, 2B: 11.93%
500	9	3.78	1A: 14.40%, 1B: 13.61%, 2A: 17.04%, 2B: 17.23%
700	15	8.84	1A: 13.59%, 1B: 13.28%, 2A: 14.52%, 2B: 14.63%
900	24	10.76	1A: 23.62%, 1B: 25.15%, 2A: 26.28%, 2B: 27.40%

be used that explicitly controls for deviations from the spatial correlation in ground motion produced by the full earthquake inventory. Second, capacity expansion to address seismic risk should be considered along with other hazards, such as hurricanes and other drivers of expansion considerations including geographic population shifts and growth. Third, the impacts on the lower voltage distribution system should also be considered, since earthquake damage to the distribution system connecting the transmission system to the customers can be extensive. Fourth, we focus on a deterministic restoration process. With sufficient observed data, uncertainty could be incorporated into restoration costs and times. Of course, this would substantially complicate the formulation and solution procedure since there would be an explosion in the number of time periods required to represent the restoration process. Fifth, we focus on physical damage to the components of large transmission system and measure the performance of the power system after the earthquake as the summation of the load shed costs and the generation cost where all units of load are assumed to be equally important. In practice, all loads are not equally important, and their relative importance does impact the scheduling of repairs. Relatedly and ideally, the analysis would more precisely quantify the impacts on end-users.

Declaration of conflicting interests

The author(s) declared no potential conflicts of interest with respect to the research, authorship, and/or publication of this article.

Funding

The author(s) disclosed receipt of the following financial support for the research, authorship, and/or publication of this article: This material is based on work supported by the National Science Foundation under collaborative awards 1735354 and 1832662. The statements, findings, and conclusions are those of the authors and do not necessarily reflect the views of the National Science Foundation.

ORCID iDs

Boyu Cheng https://orcid.org/0000-0003-2505-2483
Linda Nozick https://orcid.org/0000-0002-5629-3733
Ian Dobson https://orcid.org/0000-0001-7018-5475

Note

1. The Eastern interconnect of North America is represented by DC load flow model with 14,957 buses (nodes) that is a reduction of the East Central Area Reliability Council 2003 summer peak planning case.

References

Atkinson GM and Boore DM (1995) Ground-motion relations for eastern North America. *Bulletin of the Seismological Society of America* 85(1): 17–30.

Atkinson GM and Boore DM (2006) Earthquake ground-motion prediction equations for eastern North America. *Bulletin of the Seismological Society of America* 96(6): 2181–2205.

Bakun WH, Johnston AC and Hopper MG (2002) *Modified Mercalli Intensities (MMI) for Large Earthquakes Near New Madrid, Missouri, in 1811-1812 and Near Charleston, South Carolina, in 1886*. Washington, DC: US Department of the Interior; Reston, VA: US Geological Survey.

Baldick R, Chowdhury B, Dobson I, Dong Z, Gou B, Hawkins D, Huang H, Joung M, Kirschen D, Li F, Li J, Li Z, Liu CC, Mili L, Miller S, Podmore R, Schneider K, Sun K, Wang D, Wu Z, Zhang P, Zhang W and Zhang X (2008) Initial review of methods for cascading failure analysis in electric power transmission systems IEEE PES CAMS task force on understanding, prediction, mitigation and restoration of cascading failures. In: *Proceedings of the 2008 IEEE power and energy society general meeting—Conversion and delivery of electrical energy in the 21st century*, Pittsburgh, PA, 20–24 July, pp. 1–8. New York: IEEE.

Bialek J, Ciapessoni E, Cirio D, Cotilla-Sanchez E, Dent C, Dobson I, Henneaux P, Hines P, Jardim J, Miller S, Panteli M, Papic M, Pitto A, Quiros-Tortos J and Wu D (2016) Benchmarking and validation of cascading failure analysis tools. *IEEE Transactions on Power Systems* 31(6): 4887–4900.

Bie Z, Lin Y, Li G and Li F (2017) Battling the extreme: A study on the power system resilience. *Proceedings of the IEEE* 105(7): 1253–1266.

Birge JR and Louveaux F (2011) *Introduction to Stochastic Programming*. Berlin; Heidelberg: Springer Science + Business Media.

Bonneville Power Administration (BPA) (2020) Outage and reliability reports. Available at: https://transmission.bpa.gov/Business/Operations/Outages (accessed 12 January 2021).

Campbell KW (2003) Prediction of strong ground motion using the hybrid empirical method and its use in the development of ground-motion (attenuation) relations in eastern North America. *Bulletin of the Seismological Society of America* 93(3): 1012–1033.

Cavalieri F, Franchin P, Buriticá Cortés JAM and Tesfamariam S (2014) Models for seismic vulnerability analysis of power networks: Comparative assessment. *Computer-Aided Civil and Infrastructure Engineering* 29(8): 590–607.

Central United States Earthquake Consortium (CUSEC) (2014) MMI New Madrid earthquake. Available at: https://www.arcgis.com/home/item.html?id = 95245f40cee94d28b83cad7a83a3a8a3 (accessed 12 January 2021).

Dobson I (2012) Estimating the propagation and extent of cascading line outages from utility data with a branching process. *IEEE Transactions on Power Systems* 27(4): 2146–2155.

Dong X, Shinozuka M and Chang S. Utility power network systems. In: *Proceedings of 13th World Conference on Earthquake Engineering*; 2004. kout-2003-final-report-august-14-2003-blackout-united

Dunn WL and Shultis JK (2011) *Exploring Monte Carlo Methods*. Amsterdam: Elsevier.

Eastern Interconnection Reliability Assessment Group (ERAG) (1998) Eastern Interconnection Reliability Assessment Group. Available at: https://rfirst.org/ProgramAreas/ESP/ERAG/Pages/ERAG.aspx (accessed 12 January 2021).

Eidinger J (2009) Wenchuan earthquake impact to power systems. In: *Proceedings of the technical council on lifeline earthquake engineering conference (TCLEE'2009)*, Oakland, CA, 28 June–1 July, pp. 1–12. Reston, VA: ASCE.

Espinoza S, Poulos A, Rudnick H, de la Llera JC, Panteli M and Mancarella P (2020) Risk and resilience assessment with component criticality ranking of electric power systems subject to earthquakes. *IEEE Systems Journal* 14(2): 2837–2848.

Federal Emergency Management Agency (FEMA) (2020) *HAZUS Earthquake Model—Technical Manual*. Washington, DC: US Department of Homeland Security, FEMA.

Frankel AD, Mueller C, Barnhard T, Perkins D, Leyendecker EV, Dickman N, Hanson S and Hopper M (1996) *National seismic-hazard maps: Documentation June 1996*. Open-file report no. 96-532. Reston, VA: US Geological Survey.

Gearhart J, Brown N, Jones D, Nozick L, Romero NR and Xu N (2014) Optimization-based probabilistic consequence scenario construction for lifeline systems. *Earthquake Spectra* 30(4): 1531–1551.

Henneaux P, Ciapessoni E, Cirio D, Cotilla-Sanchez E, Diao R, Dobson I, Gaikwad A, Miller S, Papic M, Pitto A, Qi J, Samaan N, Sansavini G, Uppalapati S and Yao R (2018) Benchmarking quasi-steady state cascading outage analysis methodologies. In: *Proceedings of the 2018 IEEE international conference on probabilistic methods applied to power systems (PMAPS)*, Boise, ID, 24–28 June, pp. 1–6. New York: IEEE.

Johnston AC (1996) Seismic moment assessment of earthquakes in stable continental regions—I. Instrumental seismicity. *Geophysical Journal International* 124(2): 381–414.

Kelly-Gorham MR, Hines PDH and Dobson I (2019) Using historical utility outage data to compute overall transmission grid resilience. In: *Proceedings of the 2019 modern electric power systems conference*, Wrocław, 9–12 September, pp. 1–7. New York: IEEE.

Kelly-Gorham MR, Hines PDH, Zhou K and Dobson I (2020) Using utility outage statistics to quantify improvements in bulk power system resilience. *Electric Power Systems Research* 189: 106676.

Lagos T, Moreno R, Espinosa AN, Panteli M, Sacaan R, Ordonez F, Rudnick H and Mancarella P (2019) Identifying optimal portfolios of resilient network investments against natural hazards, with applications to earthquakes. *IEEE Transactions on Power Systems* 35(2): 1411–1421.

Liu CC (2015) Distribution systems: Reliable but not resilient? [In my view]. *IEEE Power and Energy Magazine* 13(3): 93–96.

Liu Y, Nair N-K, Renton A and Wilson S (2017) Impact of the Kaikōura earthquake on the electrical power system infrastructure. *Bulletin of the New Zealand Society for Earthquake Engineering* 50(2): 300–305.

Massie A and Watson NR (2011) Impact of the Christchurch earthquakes on the electrical power system infrastructure. *Bulletin of the New Zealand Society for Earthquake Engineering* 44(4): 425–430.

Nagarajan H, Yamangil E, Bent RV, Van Hentenryck P and Backhaus S (2016) Optimal resilient transmission grid design. In: *Proceedings of the 2016 power systems computation conference (PSCC)*, Genoa, 20–24 June, pp. 1–7. New York: IEEE.

Nazemi M, Moeini-Aghtaie M, Fotuhi-Firuzabad M and Dehghanian P (2019) Energy storage planning for enhanced resilience of power distribution networks against earthquakes. *IEEE Transactions on Sustainable Energy* 11(2): 795–806.

Noda M (2001) Disaster and restoration of electricity supply system by Hanshin-Awaji earthquake. In: *Proceedings of the seminar on earthquake disaster management of energy supply system—Chinese Taipei: Earthquake response cooperation program for energy supply systems*, Taipei, Taiwan, 5–6 September.

Nuti C, Rasulo A and Vanzi I (2007) Seismic safety evaluation of electric power supply at urban level. *Earthquake Engineering & Structural Dynamics* 36(2): 245–263.

Owen AB (2013) *Monte Carlo Theory, Methods and Examples*, pp. 10–14. https://artowen.su.domains/mc/

Papic M, Bell K, Chen Y, Dobson I, Fonte L, Haq E, Hines P, Kirschen D, Luo X, Miller SS, Samaan N, Vaiman M, Varghese M and Zhang P (2011) Survey of tools for risk assessment of cascading outages. In: *Proceedings of the 2011 IEEE power and energy society general meeting*, Detroit, MI, 24–28 July, pp. 1–9. New York: IEEE.

Petersen MD, Frankel AD, Harmsen SC, Mueller CS, Haller KM, Wheeler RL, Wesson RL, Zeng Y, Boyd OS, Perkins DM, Luco N, Field EH, Wills CJ and Rukstales KS (2008) *Documentation for the 2008 update of the United States national seismic hazard maps*. Open-file report no. 2008-1128 (May). Reston, VA: US Geological Survey.

Romero NR, Nozick LK, Dobson I, Xu N and Jones DA (2013) Transmission and generation expansion to mitigate seismic risk. *IEEE Transactions on Power Systems* 28(4): 3692–3701.

Romero NR, Nozick LK, Dobson I, Xu N and Jones DA (2015) Seismic retrofit for electric power systems. *Earthquake Spectra* 31(2): 1157–1176.

Shumuta Y (2007) Practical seismic upgrade strategy for substation equipment based on performance indices. *Earthquake Engineering & Structural Dynamics* 36(2): 209–226.

Silva W, Gregor N and Darragh R (2002) *Development of Regional Hard Rock Attenuation Relations for Central and Eastern North America*. El Cerrito, CA: Pacific Engineering and Analysis.

Stankovic A (2018) *The definition and quantification of resilience* (Prepared by the IEEE PES Industry Technical Support Task Force). Technical report no. PES-TR65, April 6. New York: IEEE.

Tavakoli B and Pezeshk S (2005) Empirical-stochastic ground-motion prediction for eastern North America. *Bulletin of the Seismological Society of America* 95(6): 2283–2296.

Toro GR, Abrahamson NA and Schneider JF (1997) Model of strong ground motions from earthquakes in central and eastern North America: Best estimates and uncertainties. *Seismological Research Letters* 68(1): 41–57.

United States Census Bureau (USCB) (2003) *Population and Housing Unit Estimates Datasets*. Available at: https://www.census.gov/programs-surveys/popest/data/data-sets.2003.html (accessed 22 January 2021).

US-Canada Power System Outage Task Force (2004) *Final Report on the August 14, 2003 Blackout in the United States and Canada: Causes and Recommendations*. https://www.energy.gov/oe/downloads/blackout-2003-final-report-august-14-2003-blackout-united-states-and-canada-causes-and

US Geological Survey (USGS) (2008a) *Data Release for the 2008 National Seismic Hazard Model for the Conterminous US*. Available at: https://data.usgs.gov/datacatalog/data/USGS:5db892f2e4b0b0c58b5a51b6 (accessed 22 January 2021).

US Geological Survey (USGS) (2008b) *NSHMP Models, Codes and Catalogs—National Seismic Hazard Mapping Project*. Available at: https://www.usgs.gov/media/images/nshmp-models-codes-catalogs-national-seismic-hazard-mapping-project (accessed 22 January 2021).

Vanzi I (1996) Seismic reliability of electric power networks: Methodology and application. *Structural Safety* 18(4): 311–327.

Vanzi I (2000) Structural upgrading strategy for electric power networks under seismic action. *Earthquake Engineering & Structural Dynamics* 29(7): 1053–1073.

Vaziri P, Davidson R, Apivatanagul P and Nozick L (2012) Identification of optimization-based probabilistic earthquake scenarios for regional loss estimation. *Journal of Earthquake Engineering* 16(2): 296–315.

Zhou K, Dobson I and Wang Z (2020) Can the Markovian influence graph simulate cascading resilience from historical outage data? In: *Proceedings of the 2020 international conference on probabilistic methods applied to power systems (PMAPS)*, Liège, 18–21 August, pp. 1–6. New York: IEEE.